Journal of Applied Pharmaceutical Science Vol. 15(07), pp 203-219, July, 2025
Available online at http://www.japsonline.com
DOI: 10.7324/JAPS.2025.231809
ISSN 2231-3354

Quorum sensing inhibitory potential and molecular docking study of lipid extract from *Xylocarpus granatum* leaves against *Pseudomonas aeruginosa*

Sumardi Sumardi[1,2], Masfria Masfria[1,3*], Mohammad Basyuni[4], Abdi Wira Septama[5]

[1]Faculty of Pharmacy, Universitas Sumatera Utara, Medan, Indonesia.
[2]Faculty of Pharmacy, Institut Kesehatan Medistra Lubuk Pakam, Lubuk Pakam, Indonesia.
[3]Department of Nanomedicine, Faculty of Pharmacy, Universitas Sumatera Utara, Medan, Indonesia.
[4]Department of Forestry, Faculty of Forestry, Universitas Sumatera Utara, Medan, Indonesia.
[5]Research Center for Pharmaceutical Ingredients and Traditional Medicine, National Research and Innovation Agency (BRIN), Kawasan Sains dan Teknologi (KST) Soekarno, Cibinong, Indonesia.

ARTICLE HISTORY

Received on: 11/12/2024
Accepted on: 20/03/2025
Available Online: 05/06/2025

Key words:
Total lipid, nonsaponifiable lipid, *X. granatum leaves*, anti-quorum sensing, molecular docking.

ABSTRACT

The quorum sensing (QS) aspect of the pathogenic *Pseudomonas aeruginosa* is a major problem in drug resistance. The development of drugs of natural origin is a therapeutic option or a lead compound in improving the weakness of antibiotics. *Xylocarpus granatum* is used as traditional medicine for the treatment of several ailments, including infectious diseases. Studies on the activity of QS have not been done much, especially the nonsaponifiable lipid compounds (NSL). The dried leaves of *X. granatum* were macerated with chloroform: methanol (2:1) for 48 hours. The filtrate was evaporated to yield total lipids (TLs), which were then saponified with 2 M KOH in 50% ethanol at 60°C and shaken for 24 hours. The n-hexane extractable portion was considered NSL. Profiling the compounds using the gas chromatography-mass spectrometry technique. Anti-QS properties were performed against *P. aeruginosa*. *In vitro*, it could inhibit growth, bactericidal, and QS activity, including swarming motility, biofilm formation, pyoverdin–pyocyanin production, and protease activity. However, TL was found to suppress virulence factors more effectively. Most NSL compounds can stop the activity of LasR, LasI, and Pseudomonas quinolone signaling receptor protein molecules, which are very important in the QS system. These studies suggest that lipid extract has potential for therapeutic management of *P. aeruginosa* infections.

INTRODUCTION

The current management of pathogenic bacterial infections is the mainstay of antibiotic therapy [1]. This therapy provides hope for potentially fatal bacterial infection conditions. However, in recent decades, the over and abuse of antibiotics as well as social and economic factors have accelerated the spread of antibiotic-resistant bacteria, causing the therapy to become ineffective. Currently, at least 700,000 people worldwide die each year due to antimicrobial resistance, while the number is expected to increase and reach 10 million by 2050 [2].

The main cause of the problem is the quorum sensing (QS) activity of bacteria. It is a key part of making bacteria more harmful by controlling the expression of genes involved in virulence, such as those that make biofilm, toxins, and antibiotic resistance [3].

Pseudomonas aeruginosa is an infection-causing bacterium that is of concern because it is a major threat to humans and has a global impact [2,4]. This bacterium could form biofilms, which is a major factor in antibiotic resistance. The study of medicinal compounds that work to inhibit the

**Corresponding Author*
Masfria Masfria, Faculty of Pharmacy, Universitas Sumatera Utara, Medan, Indonesia; Department of Nanomedicine, Faculty of Pharmacy, Universitas Sumatera Utara, Medan, Indonesia. E-mail: masfria@usu.ac.id

stages of QS an important strategy for preventing antibiotic resistance and other negative effects caused [5].

The progress of the discovery of drugs from natural resources has shown significant progress. The potential that remains to be developed is the nyirih plant (*Xylovarpus granatum*). This plant has a habitat in the tidal zone of coastal areas, beaches, or small islands, playing an important role in the surrounding aquatic ecosystem [6]. Biological activity studies include anticancer [7], antimalarial, antiviral, antifeedant, antidiabetic, antidepressant, antifungal, antioxidant [8], and antibacterial [9].

Plants primarily consist of lipids, which also possess bioactive potential for therapeutic use, particularly in the treatment of antibiotic-resistant microbial infections [10]. Even, the lipid-cell membrane vesicle hybrid has been developed and used in drug delivery systems for infectious therapy [11]. However, research related to the mechanism of anti-QS inhibition has not been widely conducted. This study focuses on the effect of lipid compounds from *Xylocarpus granatum* leaves to find potential candidates against QS activity of *P. aeruginosa* and screened based on molecular docking, drug-likeness, and toxicity prediction.

MATERIALS AND METHODS

Chemicals and media

Phosphate buffered saline (PBS) (Oxoid, United Kingdom). Vancomycin and crystal violet (Sigma-Aldrich, United Kingdom). Chloroform, methanol, KOH, and n-hexane (smartlab, Indonesia). Brain heart infusion (BHI) and agar (H-Media, India).

Preparation of lipid extract from *X. granatum*

Nyirih leaves (*X. granatum*) were obtained from the mangrove forest in Pulau Sembilan, Langkat Regency, North Sumatra, Indonesia. The plant was identified in the Medanese Laboratory of Universitas Sumatera Utara-Medan, Indonesia. Mature leaves were selected, cleaned, and dried in an oven. Then, powdered and macerated using a chloroform (2:1) mixture for 48 hours, with the extraction process repeated twice. The obtained filtrate was evaporated to yield a solid fraction, referred to as total lipid (TL). Subsequently, saponification was performed with KOH 2 M in 50% ethanol at 60°C while shaking for 24 hours. The unsaponifiable fraction was considered as the nonsaponifiable lipid (NSL), which was then partitioned using n-hexane, and subsequently referred to as the NSL [12].

Phytochemical constituent analysis

The obtained NSL was further analyzed for its chemical compound content using gas chromatography with an Agilent 7890B system coupled with a 5977A mass spectrometry detector. The analysis utilized an Agilent HP-104 5MS capillary column [(5%-phenyl)-methylpolysiloxane, 30 m × 0.25 mm I.D with a film thickness of 0.25 µm] and helium as the carrier gas at a constant flow rate of 1 ml/min. The gas chromatography-mass spectrometry system operated in splitless mode with the inlet temperature maintained at 250°C. The GC oven temperature was initially set at 40°C for 1 minute, then gradually increased to 300°C at a rate of 10°C/min and held at 300°C for 4 minutes. Component identification was performed by comparing mass spectra data and retention index values with data from the National Center for Biotechnology Information library and the NIST Chemistry WebBook. The relative amount of each identified volatile compound was quantified from the % peak area of the chromatogram [13].

Minimum inhibitory concentration (MIC) and minimum bactericidal concentration (MBC) assay

The *P. aeruginosa* cultures were each suspended, and the turbidity of the culture was adjusted with physiological NaCl solution to match the McFarland standard No. 2 (equivalent to 6 × 10^8 CFU/ml) [13,14]. Each well of a 96-well microplate was filled with 100 µl of BHI broth. Each well was then loaded with the test substances according to a serial two-fold dilution matrix. The total volume of each well was 200 µl. The positive control used was vancomycin at a concentration of 100 µg/ml [14].

The MIC was determined by identifying the lowest concentration of the test substance required to inhibit bacterial growth, observable by comparing the turbidity of the inoculum. The MBC was determined by subculturing samples from MIC and 2MIC on prepared BHI agar plates, followed by incubation for 24 hours. The sample was considered bactericidal if no bacterial growth was observed after incubation. All treatments were performed in triplicate [14].

QS assay

Biofilm formation assay

A volume of 100 µl of *P. aeruginosa* suspensions was added to the wells of a 96-well microplate containing BHIB medium and test substance solutions at concentrations of MIC and 2MIC. The plate was then incubated for 48 hours. Each well was rinsed with PBS to remove planktonic cells and purify the formed biofilm. Wells containing biofilms were stained with crystal violet (0.3%). For quantification, the crystal violet was dissolved with 95% ethanol, and the optical density was measured at a wavelength of 560 nm using a microplate reader. Each treatment was conducted in triplicate [13].

Swarming motility assay

Swarming motility activity of *P. aeruginosa* can be observed using a semisolid agar medium (0.5% w/v). The sterile swarming medium was poured into Petri dishes, and the test substances were added at concentrations of MIC and 2MIC. The medium was allowed to solidify with the lid open at room temperature for 15 minutes. Subsequently, a well was made in the center of the medium, and 50 µl of the bacterial suspension was added. The plates were incubated at 37°C for 24 hours. Each treatment was performed in triplicate [13]. The swarming motility zone was measured from the point of inoculation.

Pyoverdine, pyocyanin, and protease assay

One hundred microliters of *P. aeruginosa* cells (McFarland standard No. 2) were cultured in both the presence

and absence of TL and NSL in 2 ml of BHI broth and incubated at 37°C for 48 hours. Dimethyl sulfoxide was used as a solvent control. Following incubation, the culture was centrifuged at 10,000 rpm for 10 minutes to pellet the cells. The absorbance of pyoverdine in the cell-free supernatant was measured at 400 nm, and the pyocyanin pigment was measured at 691 nm. The cell pellets were then loaded into wells created in skim milk agar and incubated overnight at 37°C to observe zones of protease activity. Each treatment was performed in triplicate [15].

Data analysis using the two-way analysis of variance method with post hoc Tukey's multiple comparisons test (p-value = 0.05) with significance levels ≤ 0.0332 (*), ≤ 0.0021 (**), ≤ 0.0002 (***).

Molecular docking

The QS receptor proteins were obtained from the Protein Data Bank (PDB) (www.rcsb.org/pdb). The crystal structures LasR, LasI, and Pseudomonas quinolone signaling receptor (PqsR) were utilized as target receptor proteins. Amount of lipid compounds from the leaves of *X. granatum* were prepared with their 3D structures using MarvinSketch 24.1.2 software. The preparation of the receptor protein structure involved removing water molecules and selecting the appropriate chain using Open-Source PyMOL software. Hydrogen bond charges were assigned to both the ligand and receptor, and grid coordinates were determined using AutoDockTools 1.5.7. The docking of molecules was performed using AutoDock Vina. The application was run using scripts in Notepad++ and executed via the command line application Git Bash. The docking method was validated using re-docking with root mean square deviation (RMSD) parameters [16]. The docking simulation was performed using Vina 1.2.5 with the following parameters: the grid size was set to 20 × 20 × 20 grid points, with a spacing of 0.375 Å. A smoothing factor of 0.5 was applied, and the dielectric constant was set to −0.1465. The exhaustiveness of the search was adjusted to 16, with a variable spacing of 1 and a variable central processing unit count of 8. Furthermore, the simulation was conducted 10 times to ensure the reliability of the results. The simulation time ranged from 100 to 200 ns. The protonation states of the ligands are determined based on their pKa values during the preparation process, with the standard physiological pH of 7.4 (default value). The 3D and 2D visualization of the ligand-receptor complexes was done using PyMol and LigPlus v2.2 software [17]. Principal component analysis (PCA) was used to look at the binding affinity values of each compound and see which ones were moving toward the QS mechanism.

Drug-likeness prediction

All phytochemical structures are converted into the Simplified Molecular Input Line Entry System format. The drug-likeness properties were evaluated using Lipinski's Rule of Five. Prediction of physicochemical parameters and absorption, distribution, metabolism, excretion, and toxicity (ADMET) were performed using the web tool SWISSADME [18].

RESULTS AND DISCUSSION

MIC and MBC activities

Xylocarpus granatum leaves were carried directly into the habitat. The location was in Pulau Sembilan Village (Indonesia) with coordinates www.google.com/maps 4.146293,98.233795. TL had an MIC of 2.5 and an MBC of 5.0 mg/ml, while NSL showed an MIC of 2.0 and an MBC of 4.0 mg/ml. Vancomycin as a positive control, had the same MIC and MBC of 0.003 mg/ml. We have confirmed the antibacterial activity of the TL and NSL. The values are critical metrics used to evaluate the effects of antimicrobial agents, particularly in the context of QS inhibition [19]. So, this follow-up study was about how this lipid might work as a QS inhibitor for *P. aeruginosa*.

NSL had higher antibacterial activity compared to TL. However, both have much lower antibacterial activity compared to vancomycin as a control. This antibiotic was still effective at the therapeutic limit value of MIC 2 mg/ml [20].

The effectiveness of lipid and polar extracts from medicinal plants against multi drug-resistant pathogenic bacteria has been widely reported [21]. Lipids in fatty acids, sterols, monoacylglycerols, and terpenoids have been confirmed as antimicrobials extracted from plants with antibacterial potential in the last decade [22,23].

QS activities

TL and NSL significantly slowed down swarming activity, and the 2 MIC stopped *P. aeruginosa* from swarming at all (Fig. 1a). The movement pattern of the bacteria spread over the agar medium was not symmetrical (Fig. 1a). The colonies were moving in a certain direction and not evenly distributed. This bacterial pattern was known as dendritic [24]. The inhibition of swarming motility activity of NSL was better than TL, due to the concentration of lipid compounds. These changes facilitate separation with lipid compounds that do not undergo saponification, including rubberonoid compounds, steroids, terpenoids, and other compounds [25].

TL reduced biofilm formation and showed slightly better effectiveness at higher concentrations, while NSL also inhibited biofilm formation, though without a significant dose-dependent effect (Fig. 1b). Natural compounds offer a promising therapeutic strategy for inhibiting biofilms by targeting mechanisms such as QS, matrix disruption, bacterial adhesion, and biofilm dispersal, providing a safer and effective alternative to combat biofilm-associated infections [26].

TL and NSL significantly reduced the production of pyoverdine and pyocyanin, but not dependent on dose (Fig. 1c and d). The metabolites pyoverdine and pyocyanin produced by *P. aeruginosa* have an important role in its pathogenesis. It was important for pyoverdine to be present in environments low in iron, and pyocyanin makes pathogens more dangerous by creating reactive oxygen species. Protease production also plays an important role in host protein degradation, which aids in tissue invasion [27,28].

Both lipids inhibit protease activity. Even TL at 2 MIC, the pellet of sediment could not break down skim milk (Fig. 1e). Proteases, an enzyme involved in various biological processes, are necessary to break down important protein substrates in the host. They also modify a variety of biological processes and maintain the interactions between bacteria and hosts [29]. The total protease activity of *P. aeruginosa* was closely related to the incidence of multi-drug resistance [30–32]. Strategies to inhibit the total protease activity of synthetic drugs and natural materials are important [33].

The caryophyllene oxide (0.7%), vitamin E (0.7%), sitosterol (5.8%), D-limonene (0.4%), neointermedeol (0.5%), humulene epoxide II (0.4%), zingiberenol (0.7%), and α-bisabolol (1.0%) shown in Table 1 have been reported to be terpenoid derived from medicinal plants having an activity to inhibit biofilm formation, swarming motility and virulence factor of *P. aeruginosa* [34–39].

In line with this study, rose absolute extract (0.5% v/v) and phenylethyl alcohol inhibited virulence factors [40]. The monoterpenoid compounds α-terpineol (α-T) and terpinen-4-ol are active in the inhibition of pyocyanin production and total protease of *P. aeruginosa*, even the combination of the two provides a synergistic effect [41]. Besides, caryophyllene oxide has a high binding affinity value against 3C protease of hepatitis A and thymidine kinase of herpes simplex virus [42]. Besides, lipid compounds like caprilic acid, curcumin, thymol, eugenol, carvacrol, coumarin, catechin, terpinene-4-ol, linalool,

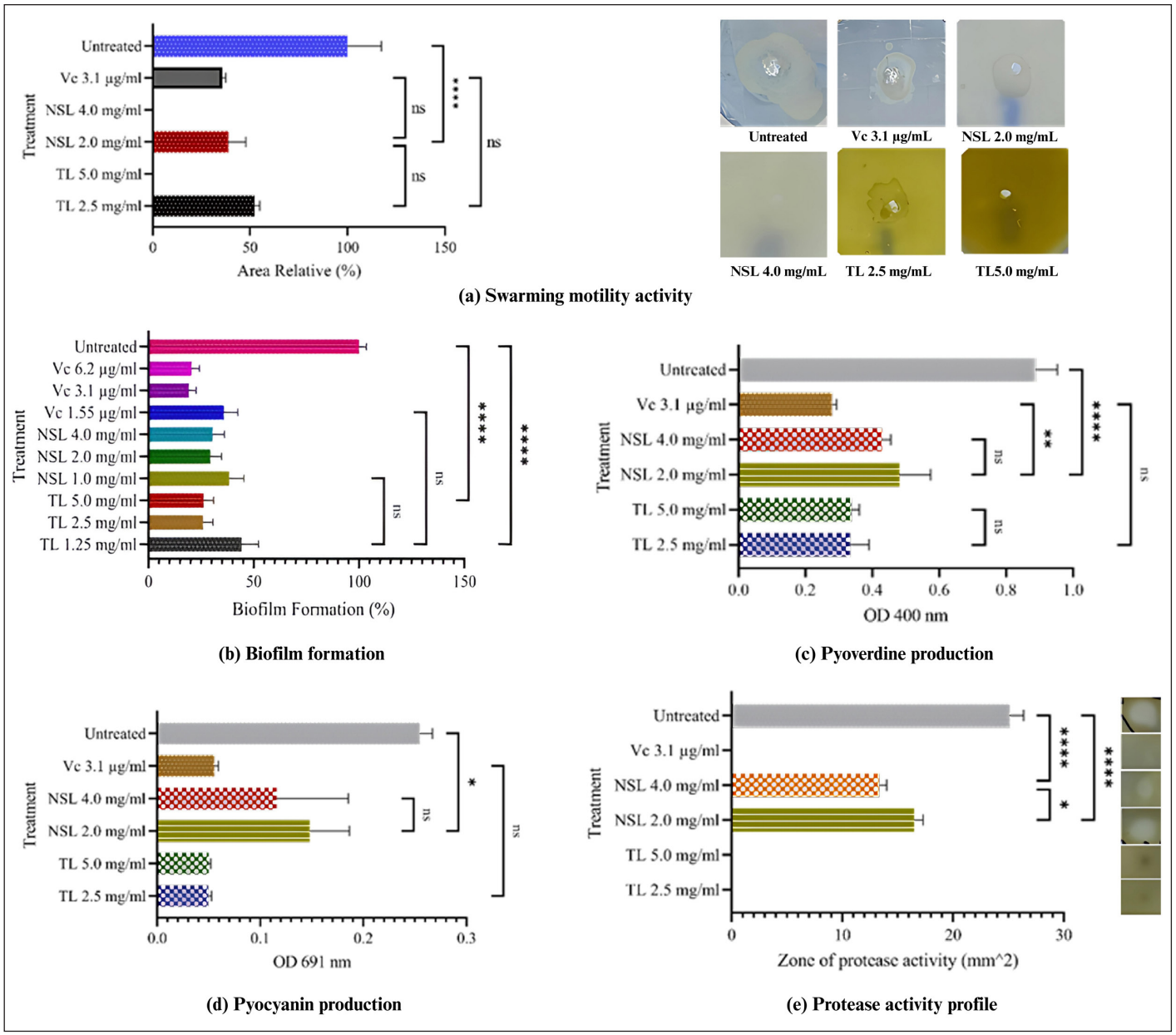

Figure 1. The role of TL and NSL on the QS activity of *P. aeruginosa.* Notes: ns: not significant, (*): significant.

Table 1. The profile of the NSL compounds in the leaves of X. *granatum*.

ID. Comp.	Name	Formula	Physicochemical properties					RC (%)	(Physicochemical properties)* (mean)*						ADMET Prediction						
									LasR		LasI		PqsR								
			HA	TPSA	nH−Acc	nH−Don	LogP		BA	LE	BA	LE	BA	LE	GI abs	BBB	P−gp Subs	CYP−1	CYP−2	Log Kp	BA
Xg1	(-)-β-Bourbonene	C15H24	15 ± 3.55	0	0	0	3.34 ± 0.28	0.2	−8.72 ± 0.07	−0.58 ± 0.005	−4.29 ± 0.004	−0.29 ± 0.000	−7.46 ± 0.120	−0.50 ± 0.008	Low	Yes	No	Yes	Yes	−4.2 ± 0.99	0.55
Xg2	(E)-2-epi-beta-caryophyllene	C15H24	15 ± 3.55	0	0	0	3.18 ± 0.27	0.2	−7.69 ± 0.05	−0.51 ± 0.004	−4.62 ± 0.075	−0.31 ± 0.005	−5.87 ± 0.066	−0.39 ± 0.004	Low	No	No	No	Yes	−4.44 ± 1.05	0.55
Xg3	(E)-β-Famesene	C15H24	15 ± 3.55	0	0	0	3.86 ± 0.33	2.1	−7.65 ± 0.03	−0.51 ± 0.002	−3.67 ± 0.122	−0.24 ± 0.008	−6.02 ± 0.108	−0.40 ± 0.007	Low	No	No	Yes	No	−3.27 ± 0.77	0.55
Xg4	1,6,10,14,18,22-Tetraco-sahexaen-3-ol, 2,6,10,15,19,23-hexam-ethyl-, (all-E)-(.+/-.)	C30H50O	31 ± 7.34	20.23 ± 1.71	1	1	6.66 ± 0.56	0.4	−10.21 ± 0.04	−0.33 ± 0.001	−3.43 ± 0.052	−0.11 ± 0.002	−6.85 ± 0.330	−0.22 ± 0.011	Low	No	No	Yes	No	−1.38 ± 0.33	0.55
Xg5	10-Iodo-2-oxa-7-thiatricyclo[4.3.1.0(3,8)] decane 7,7-dioxide	C8H11IO3S	13 ± 3.08	51.75 ± 4.28	3	0	1.52 ± 0.13	0.3	−5.67 ± 0.03	−0.44 ± 0.002	−3.80 ± 0.055	−0.29 ± 0.004	−3.99 ± 0.023	−0.31 ± 0.002	High	Yes	No	No	No	−7.42 ± 1.76	0.55
Xg6	1-Dodecanol, 3,7,11-trimethyl-	C15H32O	16 ± 3.79	20.23 ± 1.72	1	1	3.86 ± 0.33	0.2	−7.03 ± 0.22	−0.44 ± 0.013	−3.94 ± 0.094	−0.25 ± 0.006	−5.95 ± 0.235	−0.37 ± 0.015	High	Yes	Yes	No	No	−3.38 ± 0.80	0.55
Xg7	1-Hexacosene	C26H52	26 ± 6.15	0	0	0	6.89 ± 0.58	2.7	−7.50 ± 0.02	−0.29 ± 0.001	−2.64 ± 0.080	−0.10 ± 0.003	−5.45 ± 0.267	−0.21 ± 0.010	Low	No	Yes	No	No	0.09 ± 0.02	0.55
Xg8	2alpha-Butyl-3alpha-phenyl-1-azabicyclo[2.2.2]octane	C17H25N	18 ± 4.26	3.24 ± 0.27	1	0	3.4 ± 0.29	0.2	−8.37 ± 0.02	−0.46 ± 0.001	−4.16 ± 0.097	−0.23 ± 0.005	−7.08 ± 0.234	−0.39 ± 0.013	High	Yes	No	No	No	−4.67 ± 1.11	0.55
Xg9	2-Methyl-3-(3-methyl-but-2-enyl)-2-(4-methyl-pent-3-enyl)-oxetane	C15H26O	16 ± 3.79	9.23 ± 0.76	1	0	3.8 ± 0.32	0.3	−7.61 ± 0.40	−0.48 ± 0.025	−3.48 ± 0.482	−0.22 ± 0.030	−5.84 ± 0.033	−0.36 ± 0.002	High	Yes	No	No	No	−4.36 ± 1.03	0.55
Xg10	4,9-Muuroladien-15-ol	C15H24O	16 ± 3.79	20.23 ± 1.71	1	1	2.96 ± 0.25	0.2	−8.87 ± 0.33	−0.55 ± 0.021	−4.41 ± 0.084	−0.28 ± 0.005	−7.92 ± 0.025	−0.49 ± 0.002	High	Yes	No	No	No	−5.63 ± 1.33	0.55
Xg11	7-epi-trans-Sesquisabinene hydrate	C15H26O	16 ± 3.79	20.23 ± 1.71	1	1	3.38 ± 0.29	0.5	−7.92 ± 0.02	−0.49 ± 0.002	−4.20 ± 0.175	−0.26 ± 0.011	−6.09 ± 0.027	−0.38 ± 0.002	High	Yes	No	No	Yes	−4.76 ± 1.13	0.55
Xg12	8-(2-Nitrophenoxy) octan-1-ol	C14H21NO4	19 ± 4.50	75.28 ± 6.23	4	1	2.88 ± 0.24	0.2	−7.34 ± 0.13	−0.39 ± 0.007	−4.00 ± 0.295	−0.21 ± 0.016	−5.56 ± 0.197	−0.29 ± 0.010	High	Yes	No	Yes	Yes	−5.4 ± 1.28	0.55
Xg13	9,19-Cyclolanost-24-en-3-ol, (3β)	C30H50O	31 ± 7.34	20.23 ± 1.70	1	1	5.17 ± 0.44	4.7	−8.34 ± 0.02	−0.25 ± 0.001	−5.68 ± 0.179	−0.17 ± 0.005	−7.94 ± 0.063	−0.23 ± 0.002	Low	No	No	No	No	−1.96 ± 0.46	0.55

Continued

ID. Comp.	Name	Formula	Physicochemical properties					RC (%)	(Physicochemical properties)* (mean)*						ADMET Prediction						
									LasR		LasI		PqsR								
			HA	TPSA	nH−Acc	nH−Don	LogP		BA	LE	BA	LE	BA	LE	GI abs	BBB	P−gp Subs	CYP−1	CYP−2	Log Kp	BA
Xg14	Acetamide, N-tricyclo[4.3.1.1(3,8)] undec-3-yl-	C13H21NO	15 ± 3.55	29.1 ± 2.41	1	1	2.45 ± 0.21	0.9	−7.80 ± 0.01	−0.52 ± 0.001	−4.88 ± 0.122	−0.33 ± 0.008	−5.81 ± 0.017	−0.39 ± 0.001	High	Yes	No	No	No	−5.74 ± 1.36	0.55
Xg15	alpha-Curcumene	C15H22	15 ± 3.55	0	0	0	3.5 ± 0.30	3.5	−8.72 ± 0.07	−0.58 ± 0.005	−3.63 ± 0.035	−0.24 ± 0.002	−6.58 ± 0.152	−0.44 ± 0.010	Low	No	No	No	No	−3.71 ± 0.88	0.55
Xg16	Benzenemethanol, 4-(1,1-dimethylethyl)-	C11H16O	12 ± 2.84	20.23 ± 1.67	1	1	2.46 ± 0.21	0.3	5.01 ± 0.05	0.11 ± 0.001	−3.89 ± 0.006	−0.09 ± 0.000	−5.01 ± 0.027	−0.11 ± 0.001	High	Yes	No	No	No	−5.25 ± 1.24	0.55
Xg17	Benzo[h]quinoline, 2,4-dimethyl	C15H13N	16 ± 3.79	12.89 ± 1.07	1	0	2.66 ± 0.22	0.3	−10.52 ± 0.03	−0.66 ± 0.002	−5.25 ± 0.011	−0.33 ± 0.001	−9.10 ± 0.111	−0.57 ± 0.007	High	Yes	Yes	Yes	Yes	−4.58 ± 1.08	0.55
Xg18	beta-Sesquiphellandrene	C15H24	15 ± 3.55	0	0	0	3.58 ± 0.30	0.9	−8.93 ± 0.35	−0.60 ± 0.024	−3.73 ± 0.056	−0.25 ± 0.004	−6.82 ± 0.148	−0.45 ± 0.010	Low	No	No	No	Yes	−3.71 ± 0.88	0.55
Xg19	Bisacumol	C15H22O	16 ± 3.79	20.23 ± 1.69	1	1	2.87 ± 0.24	0.3	−9.93 ± 0.16	−0.62 ± 0.010	−4.92 ± 0.022	−0.31 ± 0.001	−6.38 ± 0.158	−0.40 ± 0.010	High	Yes	Yes	No	No	−4.74 ± 1.12	0.55
Xg20	Caryophylla-4(12),8(13)-dien-5α-ol	C15H24O	16 ± 3.79	20.23 ± 1.70	1	1	2.87 ± 0.24	0.3	−8.01 ± 0.02	−0.50 ± 0.001	−4.37 ± 0.053	−0.27 ± 0.003	−7.22 ± 0.024	−0.45 ± 0.001	High	Yes	No	No	Yes	−5.29 ± 1.25	0.55
Xg21	Caryophyllene	C15H24	15 ± 3.55	0	0	0	3.29 ± 0.28	1.9	−8.64 ± 0.02	−0.45 ± 0.001	−4.52 ± 0.017	−0.24 ± 0.001	−5.52 ± 0.099	−0.29 ± 0.005	Low	No	No	No	Yes	−4.44 ± 1.05	0.55
Xg22	Caryophyllene oxide	C15H24O	16 ± 3.79	12.53 ± 1.04	1	0	3.15 ± 0.27	0.7	−7.59 ± 0.11	−0.45 ± 0.006	−4.40 ± 0.094	−0.26 ± 0.006	−6.69 ± 0.042	−0.39 ± 0.002	High	Yes	No	No	Yes	−5.12 ± 1.21	0.55
Xg23	cis-β-Farnesene	C15H24	15 ± 3.55	0	0	0	3.86 ± 0.33	0.2	−7.61 ± 0.13	−0.51 ± 0.009	−3.22 ± 0.046	−0.21 ± 0.003	−6.41 ± 0.139	−0.43 ± 0.009	Low	No	No	Yes	No	−3.27 ± 0.77	0.55
Xg24	Copaene	C15H24	15 ± 3.55	0	0	0	3.4 ± 0.29	1.3	−8.13 ± 0.01	−0.54 ± 0.001	−4.60 ± 0.060	−0.31 ± 0.004	−7.13 ± 0.020	−0.48 ± 0.001	Low	Yes	No	Yes	Yes	−4.37 ± 1.03	0.55
Xg25	Cycloartenol acetate	C32H52O2	34 ± 8.05	26.3 ± 2.18	2	0	5.35 ± 0.45	0.3	−6.10 ± 0.11	−0.18 ± 0.003	−5.58 ± 0.142	−0.16 ± 0.004	−7.73 ± 0.100	−0.23 ± 0.003	Low	No	No	No	No	−1.81 ± 0.43	0.55
Xg26	Cyclohexane, 1-ethenyl-1-methyl-2,4-bis(1-methylethenyl)-, [1S-(1α,2β,4β)]	C15H24	15 ± 3.55	0	0	0	3.4 ± 0.29	0.4	−8.12 ± 0.10	−0.54 ± 0.007	−4.24 ± 0.025	−0.28 ± 0.002	−6.91 ± 0.068	−0.46 ± 0.005	Low	No	No	No	Yes	−3.75 ± 0.89	0.55

Continued

ID. Comp.	Name	Formula	Physicochemical properties					RC (%)	(Physicochemical properties)* (mean)*						ADMET Prediction						
									LasR		LasI		PqsR								
			HA	TPSA	nH−Acc	nH−Don	LogP		BA	LE	BA	LE	BA	LE	GI abs	BBB	P−gp Subs	CYP−1	CYP−2	Log Kp	BA
Xg27	cyclosativene	C15H24	15 ± 3.55	0	0	0	3.24 ± 0.27	0.9	−8.66 ± 0.01	−0.58 ± 0.001	−4.37 ± 0.081	−0.29 ± 0.005	−6.24 ± 0.040	−0.42 ± 0.003	Low	Yes	No	Yes	Yes	−4.09 ± 0.97	0.55
Xg28	Diazene, bis(4-butoxyphenyl)-, 1-oxide	C20H26N2O3	25 ± 5.92	59.57 ± 4.93	4	0	4.39 ± 0.37	0.4	−8.55 ±0.09	−0.34 ± 0.004	−4.69 ± 0.042	−0.19 ± 0.002	−5.77 ± 0.155	−0.23 ± 0.006	High	No	No	Yes	Yes	−4.42 ± 1.05	0.55
Xg29	Dihydroactinidiolide	C11H16O2	13 ± 3.08	26.3 ± 2.18	2	0	2.29 ± 0.19	0.9	−7.14 ±0.01	−0.55 ± 0.001	−4.43 ± 0.034	−0.34 ± 0.003	−6.63 ± 0.150	−0.51 ± 0.012	High	Yes	No	No	No	−5.87 ± 1.39	0.55
Xg30	D-Limonene	C10H16	10 ± 2.37	0	0	0	2.72 ± 0.23	0.4	−7.04 ±0.08	−0.70 ± 0.008	−3.81 ± 0.038	−0.38 ± 0.004	−6.31 ± 0.072	−0.63 ± 0.007	Low	Yes	No	No	No	−3.89 ± 0.92	0.55
Xg31	Eicosane	C21H44	21 ± 4.97	0	0	0	5.85 ± 0.49	0.5	−7.15 ±0.06	−0.36 ± 0.003	−2.65 ± 0.048	−0.13 ± 0.002	−5.37 ± 0.214	−0.27 ± 0.011	Low	No	No	Yes	No	−0.31 ± 0.07	0.55
Xg32	Epicubenol	C15H26O	16 ± 3.79	20.23 ± 1.69	1	1	3.24 ± 0.27	1.0	−8.53 ±0.09	−0.53 ± 0.006	−4.21 ± 0.029	−0.26 ± 0.002	−7.37 ± 0.120	−0.46 ± 0.007	High	Yes	No	No	Yes	−5.03 ± 1.19	0.55
Xg33	Ethanamine, 2,2-diethoxy	C8H19NO2	11 ± 2.60	30.49 ± 2.52	3	1	2.7 ± 0.23	0.3	−4.65 ±0.05	−0.52 ± 0.006	−2.74 ± 0.040	−0.30 ± 0.004	−3.60 ± 0.058	−0.40 ± 0.006	High	Yes	No	No	No	−6.74 ± 1.59	0.55
Xg34	Ethyl 2,2-diethoxypropionate	C9H18O4	13 ± 3.08	44.76 ± 3.71	4	0	2.92 ± 0.25	0.2	−5.02 ±0.01	−0.39 ± 0.001	−3.51 ± 0.133	−0.27 ± 0.010	−4.60 ± 0.111	−0.35 ± 0.009	High	Yes	No	No	No	−6.56 ± 1.55	0.55
Xg35	Farnesylacetone	C18H30O	19 ± 4.50	17.07 ± 1.41	1	0	3.67 ± 0.31	0.4	−8.60 ±0.08	−0.45 ± 0.004	−4.06 ± 0.053	−0.21 ± 0.003	−6.68 ± 0.076	−0.35 ± 0.004	High	No	No	Yes	No	−3.95 ± 0.93	0.55
Xg36	Fitone	C18H36O	19 ± 4.50	17.07 ± 1.41	1	0	4.39 ± 0.37	3.4	−7.53 ± 0.06	−0.40 ± 0.003	−3.58 ± 0.220	−0.19 ± 0.012	−5.75 ± 0.091	−0.30 ± 0.005	High	No	Yes	No	No	−3 ± 0.71	0.55
Xg37	Ginsenol	C15H26O	16 ± 3.79	20.23 ± 1.67	1	1	2.93 ± 0.25	1.1	−7.21 ±0.08	−0.45 ± 0.005	−4.43 ± 0.010	−0.28 ± 0.001	−5.31 ± 0.130	−0.33 ± 0.008	High	Yes	No	No	No	−4.81 ± 1.14	0.55
Xg38	Hexadecane	C16H34	16 ± 3.79	0	0	0	4.67 ± 0.39	0.2	−6.57 ±0.07	−0.41 ± 0.004	−2.64 ± 0.071	−0.17 ± 0.004	−4.97 ± 0.053	−0.31 ± 0.003	Low	No	No	Yes	No	−1.8 ± 0.43	0.55
Xg39	Humulene	C15H24	15 ± 3.55	0	0	0	3.27 ± 0.28	0.9	−8.23 ±0.01	−0.55 ± 0.001	−4.43 ± 0.019	−0.30 ± 0.001	−6.98 ± 0.220	−0.47 ± 0.015	Low	No	No	No	No	−4.32 ± 1.02	0.55

Continued

ID. Comp.	Name	Formula	Physicochemical properties					RC (%)	(Physicochemical properties)* (mean)*						ADMET Prediction						
									LasR		LasI		PqsR								
			HA	TPSA	nH−Acc	nH−Don	LogP		BA	LE	BA	LE	BA	LE	GI abs	BBB	P−gp Subs	CYP−1	CYP−2	Log Kp	BA
Xg40	Humulene epoxide II	C15H24O	16 ± 3.79	12.53 ± 1.04	1	0	3.11 ± 0.26	0.4	−8.18 ±0.02	−0.51 ± 0.001	−4.24 ± 0.050	−0.26 ± 0.003	−5.19 ± 0.170	−0.32 ± 0.011	High	Yes	No	No	No	−4.91 ± 1.16	0.55
Xg41	Isophytol	C20H40O	21 ± 4.97	20.23 ± 1.68	1	1	4.88 ± 0.41	0.7	−7.78 ±0.25	−0.37 ± 0.012	−3.52 ± 0.275	−0.17 ± 0.013	−5.92 ± 0.193	−0.28 ± 0.009	Low	No	Yes	No	No	−2.55 ± 0.60	0.55
Xg42	Isospathulenol	C15H24O	16 ± 3.79	20.23 ± 1.69	1	1	2.89 ± 0.24	0.7	−9.32 ±0.16	−0.58 ± 0.010	−4.65 ± 0.009	−0.29 ± 0.001	−7.84 ± 0.034	−0.49 ± 0.002	High	Yes	No	No	No	−5.78 ± 1.37	0.55
Xg43	Naphthalene	C10H8	10 ± 2.37	0	0	0	1.99 ± 0.17	1.5	−7.48 ±0.06	−0.75 ± 0.006	−3.65 ± 0.005	−0.37 ± 0.001	−6.46 ± 0.013	−0.65 ± 0.001	Low	Yes	No	Yes	No	−4.74 ± 1.12	0.55
Xg44	Naphthalene, 1,2,4a,5,6,8a-hexahydro-4,7-dimethyl-1-(1-methylethyl)	C15H24	15 ± 3.55	0	0	0	3.38 ± 0.29	0.2	−8.25 ±0.10	−0.55 ± 0.007	−4.48 ± 0.006	−0.30 ± 0.000	−6.17 ± 0.024	−0.41 ± 0.002	Low	No	No	No	Yes	−4.65 ± 1.10	0.55
Xg45	n-Butyl palmitate	C20H40O2	22 ± 5.21	26.3 ± 2.18	2	0	5.39 ± 0.46	0.2	−9.44 ±0.06	−0.43 ± 0.003	−5.48 ± 0.043	−0.25 ± 0.002	−7.42 ± 0.023	−0.34 ± 0.001	Low	No	No	Yes	No	−2.04 ± 0.48	0.55
Xg46	Neointermedeol	C15H26O	16 ± 3.79	20.23 ± 1.68	1	1	3.1 ± 0.26	0.5	−9.34 ±0.02	−0.58 ± 0.001	−4.48 ± 0.008	−0.28 ± 0.000	−7.20 ± 0.119	−0.45 ± 0.007	High	Yes	No	No	Yes	−4.48 ± 1.06	0.55
Xg47	Neophytadiene	C20H38	20 ± 4.73	0	0	0	5.05 ± 0.43	0.5	−7.80 ±0.20	−0.39 ± 0.010	−3.21 ± 0.193	−0.16 ± 0.010	−6.14 ± 0.102	−0.31 ± 0.005	Low	No	Yes	No	No	−1.17 ± 0.28	0.55
Xg48	N-hydroxy-N'-[2-(trifluoromethyl) phenyl]pyridine-3-carboximidamide	C13H10F3N3O	20 ± 4.73	57.51 ± 4.76	6	2	1.99 ± 0.17	0.7	−9.12 ±0.22	−0.46 ± 0.011	−4.95 ± 0.074	−0.25 ± 0.004	−6.86 ± 0.456	−0.34 ± 0.023	High	Yes	No	No	No	−6.34 ± 1.50	0.55
Xg49	Octadecane, 3-methyl-	C19H40	19 ± 4.50	0 ± 0.00	0	0	5.31 ± 0.45	4.0	−7.22 ±0.10	−0.38 ± 0.005	−2.79 ± 0.303	−0.15 ± 0.016	−5.68 ± 0.080	−0.30 ± 0.004	Low	No	No	No	No	−0.68 ± 0.16	0.55
Xg50	Olean-12-en-3-ol, acetate, (3β)	C32H52O2	34 ± 8.05	26.3 ± 2.18	2	0	5.19 ± 0.44	2.3	−3.72 ±0.03	−0.11 ± 0.001	−6.11 ± 0.072	−0.18 ± 0.002	−6.89 ± 0.306	−0.20 ± 0.009	Low	No	No	No	No	−2.25 ± 0.53	0.55
Xg51	sesquithujene	C15H24	15 ± 3.55	0	0	0	3.66 ± 0.31	0.2	−8.90 ±0.03	−0.59 ± 0.002	−3.90 ± 0.187	−0.26 ± 0.012	−7.04 ± 0.016	−0.47 ± 0.001	Low	No	No	No	Yes	−4.12 ± 0.97	0.55
Xg52	Torulosol	C20H34O2	22 ± 5.21	40.46 ± 3.35	2	2	3.93 ± 0.33	1.3	−7.61 ±0.29	−0.35 ± 0.013	−4.58 ± 0.017	−0.21 ± 0.001	−6.95 ± 0.315	−0.32 ± 0.014	High	Yes	No	No	Yes	−5.11 ± 1.21	0.55

Continued

ID. Comp.	Name	Formula	Physicochemical properties						(Physicochemical properties)* (mean)*						ADMET Prediction						
									LasR		LasI		PqsR								
			HA	TPSA	nH−Acc	nH−Don	LogP	RC (%)	BA	LE	BA	LE	BA	LE	GI abs	BBB	P−gp Subs	CYP−1	CYP−2	Log Kp	BA
Xg53	trans-Sesquisabinene hydrate	C15H26O	16 ± 3.79	20.23 ± 1.67	1	1	3.38 ± 0.29	0.9	−7.98 ±0.03	−0.50 ± 0.002	−4.51 ± 0.027	−0.28 ± 0.002	−6.73 ± 0.289	−0.42 ± 0.018	High	Yes	No	No	Yes	−4.76 ± 1.13	0.55
Xg54	trans-α-Bergamotene	C15H24	15 ± 3.55	0	0	0	3.52 ± 0.30	0.3	−8.04 ±0.09	−0.54 ± 0.006	−4.10 ± 0.230	−0.27 ± 0.015	−6.45 ± 0.198	−0.43 ± 0.013	Low	No	No	No	Yes	−2.97 ± 0.70	0.55
Xg55	Vitamin E	C29H50O2	31 ± 7.34	29.46 ± 2.44	2	1	5.92 ± 0.50	0.7	−11.22 ±0.03	−0.36 ± 0.001	−3.63 ± 0.162	−0.12 ± 0.005	−7.79 ± 0.417	−0.25 ± 0.013	Low	No	Yes	No	No	−1.33 ± 0.31	0.55
Xg56	Zingiberenol	C15H26O	16 ± 3.79	20.23 ± 1.62	1	1	3.41 ± 0.29	0.7	−7.86 ±0.03	−0.49 ± 0.002	−4.02 ± 0.012	−0.25 ± 0.001	−7.38 ± 0.025	−0.46 ± 0.002	High	Yes	No	No	No	−4.63 ± 1.10	0.55
Xg57	α-Bisabolol	C15H26O	16 ± 3.79	20.23 ± 1.64	1	1	3.46 ± 0.29	1.0	−9.29 ±0.12	−0.58 ± 0.008	−4.42 ± 0.071	−0.28 ± 0.004	−6.63 ± 0.208	−0.41 ± 0.013	High	Yes	No	No	No	−4.97 ± 1.18	0.55
Xg58	α-Cadinol	C15H26O	16 ± 3.79	20.23 ± 1.61	1	1	3.15 ± 0.27	0.9	−9.30 ±0.15	−0.58 ± 0.009	−4.59 ± 0.024	−0.29 ± 0.001	−7.61 ± 0.153	−0.48 ± 0.010	High	Yes	No	No	Yes	−5.29 ± 1.25	0.55
Xg59	α-Calacorene	C15H20	15 ± 3.55	0	0	0	3.12 ± 0.26	0.3	−9.74 ±0.01	−0.65 ± 0.001	−4.30 ± 0.096	−0.29 ± 0.006	−7.95 ± 0.018	−0.53 ± 0.001	Low	No	No	No	No	−4.39 ± 1.04	0.55
Xg60	α-Farnesene	C15H24	15 ± 3.55	0	0	0	3.89 ± 0.33	0.2	−8.68 ±0.02	−0.58 ± 0.002	−3.77 ± 0.201	−0.25 ± 0.013	−6.64 ± 0.139	−0.44 ± 0.009	Low	No	No	Yes	No	−3.2 ± 0.76	0.55
Xg61	γ-Muurolene	C15H24	15 ± 3.55	0	0	0	3.39 ± 0.29	0.8	−7.87 ±0.01	−0.52 ± 0.001	−4.33 ± 0.035	−0.29 ± 0.002	−7.81 ± 0.167	−0.52 ± 0.011	Low	No	No	No	Yes	−4.49 ± 1.06	0.55
Xg62	γ-Sitosterol	C29H50O	30 ± 7.10	20.23 ± 1.64	1	1	4.79 ± 0.41	5.8	−10.85 ±0.06	−0.36 ± 0.002	−5.31 ± 0.087	−0.18 ± 0.003	−8.06 ± 0.183	−0.27 ± 0.006	Low	No	No	No	No	−2.2 ± 0.52	0.55
Xg63	τ-Muurolol	C15H26O	16 ± 3.79	20.23 ± 1.67	1	1	3.07 ± 0.26	0.5	−8.94 ±0.07	−0.56 ± 0.005	−4.66 ± 0.012	−0.29 ± 0.001	−7.59 ± 0.018	−0.47 ± 0.001	High	Yes	No	No	No	−5.29 ± 1.25	0.55
	Vancomycin (control positif)								113.54 ± 0.60	1.12 ± 0.01	−5.45 ± 0.03	−0.05 ± 0.00	3.16 ± 0.02	0.03 ± 0.00							

Note. *) = number of repetitions: 6 times; TPSA = topological polar surface area; HA = heavy atom; nH-Acc = number H-bond acceptors; nH-Don = number H-bond donors; BA = binding affinity; LE = ligan efficiency; GI abs = gastrointestinal absoption; BBB = blood-brain barier; P-gp Subs = P glycoprotein substrate; CYP-1 = CYP1A2 inhibitor; CYP-2 = CYP2C19 inhibitor; BA = bioavaibility score.

pinene, cinnamaldehyde, linoleic acid, saponin, and geraniol are confirmed to be used in therapies for *P. aeruginosa* biofilms [23,43].

NSL showed stronger potential compared with TL. This was evidenced by smaller MIC, MBC, and swarming zone values. However, TL was greater in inhibiting biofilm formation, pyoverdine and pyocyanin production, and protease activity. This suggests that these lipids were antimicrobial agents but needed a concentration of certain active compounds or a combination with other agents to reach higher effectiveness.

Molecule docking of the phytochemistry and LasR, LasI, and PqsR protein interaction

A total of 63 compounds (Table 1) were identified from the NSL of *X. granatum* leaves, some of which have been confirmed to be active against QS mechanisms. In this study, virtual screening was conducted. The proteins used as receptors are enzymes that play an important role in QS activity, namely LasR, LasI, and PqsR. The performance of compounds with different shapes and functional groups affects how they interact with the receptor's amino acid residues in both hydrophobic and hydrophilic ways [44]. Molecular docking has had a great contribution to science-medicine research and has a lot of potential to generate new drugs for the treatment of diseases [45].

The LasR protein in the form of a 3D crystal structure was obtained (PDB ID: 6D6D). This protein has a resolution of 1.7 A with 2 homologous chains. Chain A with a sequence length of 169 was selected as the receptor in the docking analysis process. Re-docking analysis with 2,4-dibromo-6-{[(2-nitrobenzene-1-carbonyl) amino] methyl}phenyl 2-cyanobenzoate (FY7) as the default ligand and grid area at center coordinates (15.706, 5.487, 14.649) obtained binding affinity value of −20.72 kcal/mol and RMSD value of 0.3092 Å.

FY7 ligand works as an antagonist against the receptor, causing down regulation of pyocyanin virulence phenotype and biofilm formation [46]. Based on the binding affinity values, 62 out of 63 compounds have a score of −3 kcal/mol and the potential to be active candidate compounds, except for Xg16 (Table 1) which requires large energy to bind to the LasR receptor binding site. 2D illustration of the top ten ligands selected with the LasR protein complex are

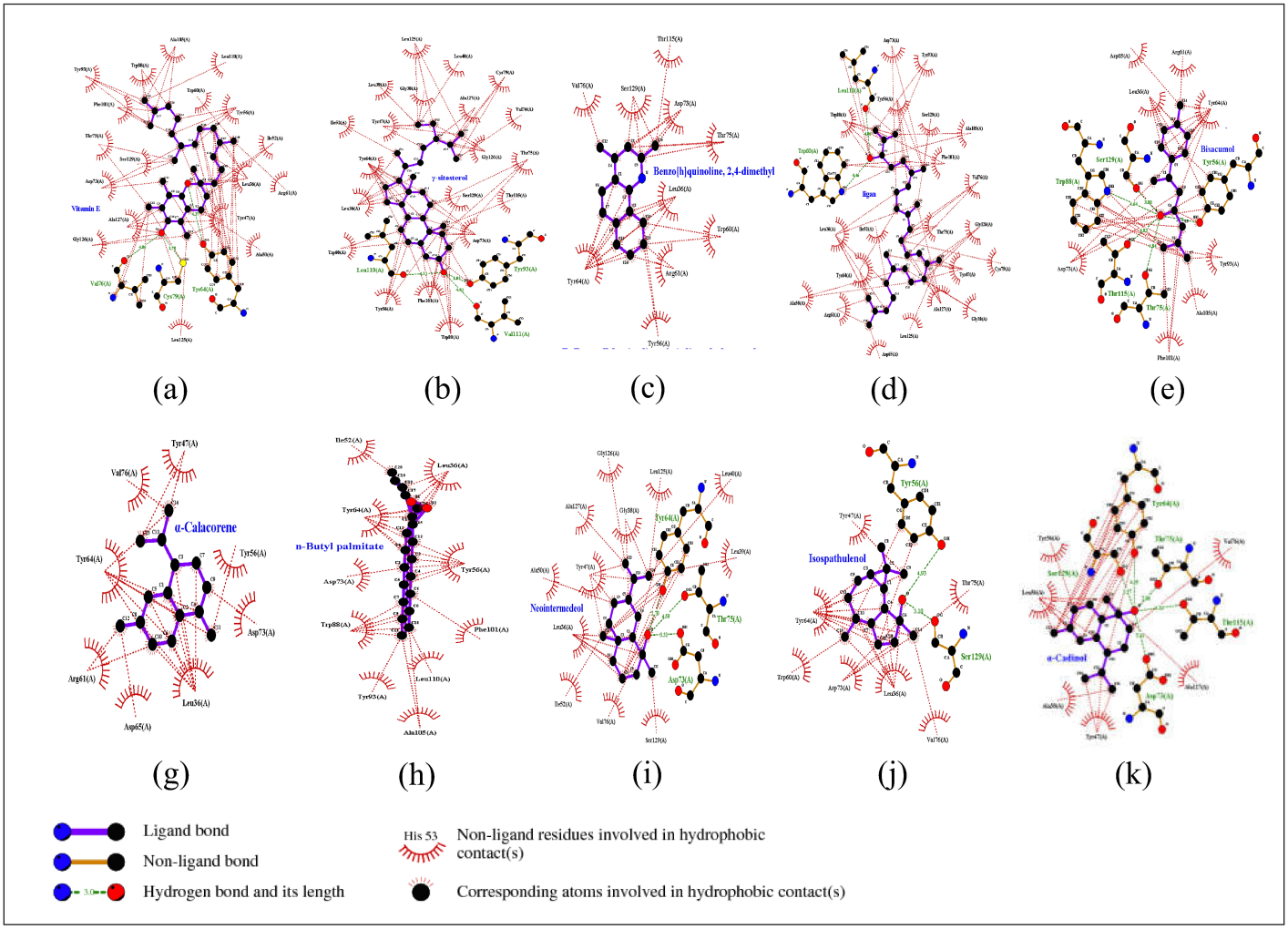

Figure 2. Visualization and interaction 2D with amino acids of LasR protein (PDB ID: 6D6D chain A) with 10 compounds selected from NSL of *X. granatum* leaves. (a) Xg55; (b) Xg62; (c) Xg17; (d) Xg4; (e) Xg19; (f) Xg59; (g) X45; (h) Xg46; (i) Xg42; (j) Xg58.

shown in Figure 2 and amino acid residue interactions in Table 2.

Leu36 was found in all complexes, which suggests that it is an important part of the active site that binds ligands through hydrophobic interactions. Additionally, Tyr56, Asp73, Val76, and Tyr64 appear in 7 to 9 complexes, presumably playing a role in forming π–π interactions and electrostatic stabilization. Tyr64, Ser129, and Thr75, on the other hand, form

Table 2. The interaction of LasR receptor amino acid residues with top 10 compounds.

ID Comp.	Hydrophobic bonds	Hydrogen bonds
Xg55	Leu125, Ala50, Tyr47, Arg61, Leu36, Ile52, Tyr56, Trp60, leu110, Ala105, Trp88, Tyr93, Phe101, Thr75, Ser129, Asp73, Ala127, Gly126)	Tyr64, Cys79, Val176
Xg62	Leu25, Leu40, Leu39, Gly38, Ala127, Val76, Cys79, Thr75, Gly126, Ser129, Thr115, Asp73, Trp98, Phe101, Tyr56, Leu36, Trp60, Tyr64, Tyr47, Ile52)	Tyr93, Val111
Xg17	Thr115, Val76, Ser129, Asp73, Thr75, Leu36, Trp60, Arg61, Tyr56, Tyr64	-
Xg4	Leu110, Tyr56, Trp88, Trp60, Asp73, Tyr93, Ser129, Ala105, Phe101, Val76, Thr75, Gly126, Ala127, Gly38, Leu125, Ala50, Arg61, Leu36, Tyr64, Ala50, Arg61	Trp60, Leu110
Xg19	Asp65, Arg61, Leu36, Tyr64, Asp73, Ala105, Phe101, Tyr93	Thr75, Thr115, Tyr56, Ser129, Trp88
Xg59	Tyr64, Val76, Tyr47, Tyr56, Asp73, Leu36, Asp65, Arg61	-
Xg45	Ile52, Leu36, Tyr64, Tyr56, Asp73, Trp88, Tyr93, Leu110, Phe101, Ala105	-
Xg46	Gly126, Ala127, Gly38, Leu25, Leu40, Leu39, Ser129, Val76, Ile52, Leu36, Ala50, Tyr47	Tyr64, Asp73, Thr75
Xg42	Tyr47, Tyr64, Trp60, Asp73, Leu36, Val76, Thr75	Tyr56, Ser129
Xg58	Leu36, Tyr56, Val76, Ala127, Ala50, Tyr47	Asp73, Thr115, Thr75, Tyr64, Ser129

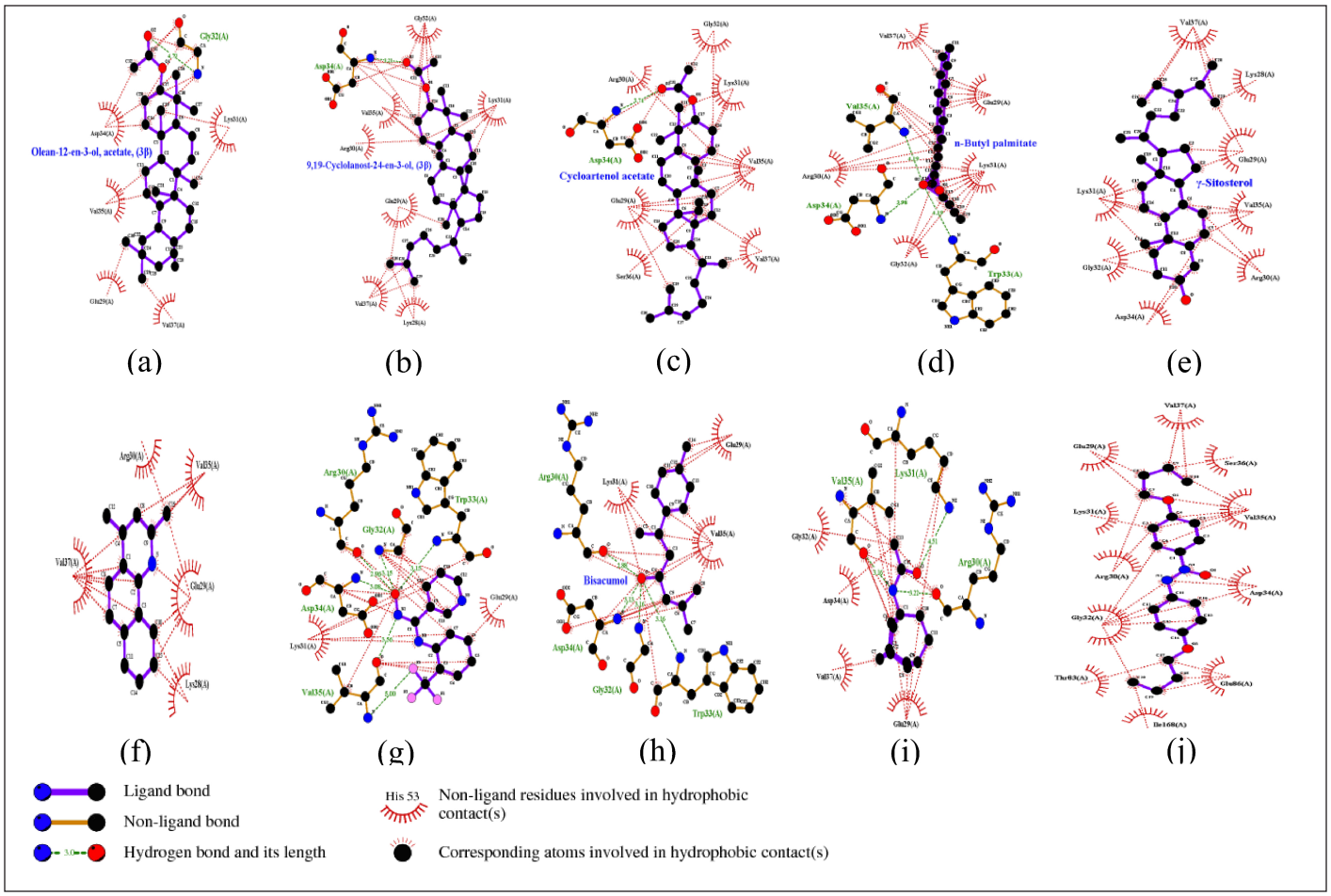

Figure 3. Visualization and interaction 2D with amino acids of LasI protein (PDB ID: 1RO5) with 10 compounds selected from NSL of *X. granatum* leaves. (a) Xg50; (b) Xg13; (c) Xg25; (d) Xg45; (e) Xg52; (f) Xg17; (g) Xg48; (h) Xg19; (i) Xg14; (j) Xg28.

hydrogen bonds that contribute to proton donation or acceptance as well as ligand stability at the active site.The 3D structure of the LasI protein was (PDB ID: 1RO5). The crystal structure of the protein has a resolution of 2.30 Å and the A chain was selected among 5 homologous chains with a sequence length of 201. Re-docking analysis with sulfate ion ($SO4^{-2}$) as the default ligand and grid area at center coordinates (55.591, −3.206, and −3.416) obtained a binding affinity value of −3.243 kcal/mol and RMSD value of 14.14 Å. The presence of ion sulfate may be attributed to the ion's small size and high mobility within the binding site. The molecular shape is a regular tetrahedron, but it can bend and take on different binding poses depending on its surroundings, which can lead to bigger deviations [47]. Despite this, the analysis remains valid if the primary interactions at the binding site are preserved, and the biological relevance of the sulfate ion's binding was maintained.

The sulfate ions can inhibit the formation of co-crystals between LasI protein and the substrate 3-oxo-C12-acyl-carrier protein (acyl-ACP) in producing 3-oxo-C12-acyl-homoserine lactone (AHL) [48]. These compounds are autoinducers in the pathogenesis process of *P. aeruginosa*. Overall, 63 compounds can be candidates to inhibit the LasI enzyme. The illustration of the 2D top 10 ligan-LasI protein complex has a higher ability shown in Figure 3 and the interactions of amino acid residues in Table 3. Val37, Lys31, Glu29, Val35, Asp34, and Gly32 were crucial for most complexes, contributing to both hydrophobic and hydrogen bond stability, while Trp33 played a role in forming stable π-interactions.The 3D structure of the PqsR protein (PDB ID: 7P4U). The crystal structure of the protein has a resolution of 2.74 Å and an A chain with a sequence length of 229. Re-docking analysis with {N}-[[2-(3-chloranyl-4-propan-2-yloxy-phenyl)pyrimidin-5-yl]methyl]-2-(trifluoromethyl)pyridin-4-amine (5N9) as the default ligand and grid area at center coordinates (−52.684, 1.852, −10.280) obtained RMSD value of 0.3062 Å and binding affinity of −12.58 kcal/mol. Generally, all 63 ligands from NSL (Table 1) good affinity category for this protein. Illustration 2D 10 ligan selected-PqsR protein complex that has a higher affinity (Fig. 4) and amino acid residues interaction in the binding site region (Table 4). Leu207, Ile236, and Thr265 Likely a core-stabilizing residue from hydrophobic bonds and central to binding pocket stabilization. Besides Leu197, Ser196, and Leu207 may be significant contributors to hydrogen bonds' specificity.PqsR is known as a regulator of multi-virulence factors (MvfR) and is also known as a regulator of MvfR which is important in QS mechanism. Compound 5N9 is a strong ligand and is recommended as a potential pyrimidine derivative compound in inhibiting the PqsR enzyme and has good solubility [49].

Chemometric analysis using the PCA method of the binding affinity value of the interaction of each ligand. The scatter plots of data have been calculated as principal component (PC) values in the form of 2-dimensional (Fig. 5a) and 3-dimensional plots (Fig. 5b).

PC1 explained 61.42% of the total variation and PC2 explained 27.25% of the total variation in the data. These two major components account for 88.67% of the variation in the data, sufficiently elucidating the data structure in two dimensions. Most of the samples were close to the plot's center, which meant they had similar traits based on the two main factors. Samples that were farther away from the ellipse, on the other hand, had different traits [50]. There were some outliers (Fig. 5a) separated from the ellipse line (pink), namely compounds Xg16, Xg33, and Xg50 have different characteristics from most other samples. The data distributed in 3D form (Fig. 5b) also indicates that most of the compounds are distributed along a single dimension; however, several compounds are separated from the main cluster.

Based on the tendency of data with large PC1 and PC2 values (Fig. 5), the compounds distributed in the middle of the dimensional population have the potential as candidate compounds that inhibit LasI, LasR, and PqsR enzymes with the assumption that they have good affinity for the three enzymes.

These results indicate that these compounds have great potential as QS inhibitory agents, but further in-depth studies are needed for the isolation and combination of these compounds to confirm the real mechanism of QS inhibition and its application in the development of more effective antibacterial therapies.

These findings indicate that the compounds, particularly those located centrally in the PCA plot, show significant potential as QS inhibitory agents, likely possessing strong affinities for the three enzymes. However, the results emphasize the necessity for further detailed studies to isolate and combine these compounds, confirm their precise

Table 3. The interaction of LasI receptor amino acid residues with top ten compounds.

ID Comp.	Hydrophobic bonds	Hydrogen bonds
Xg50	Val37, Glu29, Lys31, Asp34, Val35	Gly32
Xg13	Val37, Lys28, Glu29, Lys31, Arg30, Val35, Gly32	Asp34
Xg25	Val35, Val37, Lys31, Gly32, Arg30, Glu29, Ser36	Asp34
Xg45	Gly32, Lys31, Glu29, Val37, Arg30	Trp33, Val35, Asp34
Xg52	Arg30, Val35, Glu29, Lys28, Val37, Lys31, Gly32, Asp34	-
Xg17	Arg30, Val35, Glu29, Lys28, Val37	-
Xg48	Lys31, Glu29	Arg30, Trp33, Val35, Asp34, Gly32
Xg19	Lys31, Glu29, Val35	Trp33, Arg30, Asp34, Gly32
Xg14	Gly32, Asp34, Val37, Glu29	Val35, Lys31, Arg30
Xg28	Ile168, Glu86, Asp34, Val35, Ser36, Val37, Glu29, Lys31, Arg30, Gly32, Thr83	-

mechanisms of QS inhibition, and assess their potential for developing more effective antibacterial therapies. The PCA loading values strongly support prioritizing certain compounds, especially those with high contributions to both PC1 and PC2, such as Xg34 (Ethyl 2,2-diethoxypropionate), Xg6 (1-Dodecanol, 3,7,11-trimethyl), Xg12 (8-(2-Nitrophenoxy) octan-1-ol), Xg37 (Ginsenol), Xg21 (Caryophyllene), Xg11 (7-epi-trans-Sesquisabinene hydrate), and Xg29 ((E)-2-epi-beta-caryophyllene), as promising candidates for future QS inhibition research.

Three major QS systems in *P. aeruginosa*, two of which use AHLs as signal molecules, are called the *Las* system and the *Rhl* system, respectively. In addition, there is the *Pqs* system, which is interrelated with the other two systems. All these QS systems are closely interconnected and do not stand alone [51]. These three systems together form a complicated and hierarchical coordination. The mechanism of the QS system formed by *P. aeruginosa* has been well understood.

The lipid compounds present in *X. granatum* leaves have been selected for the 10 compounds with the highest affinity with each receptor. These results provide new insights into the metabolic mechanisms of microorganisms and the potential application of lipids in the control of bacterial infections. Furthermore, it should expect to be prioritized in subsequent studies as a marker or lead compound in drug development.

Xg17 and Xg62 emerged as ligands with high affinity to all three receptors (LasR, LasI, and PqsR). Whereas compounds with affinity to 2 receptors, including Xg13 and Xg25 interacted with both PqsR and LasI receptors. Xg42, Xg55, Xg58, and Xg59 have an affinity to LasR and PqsR. While Xg19 and Xg45 interacted with both LasR and LasI. These ten compounds have potential as candidate drugs and lead compounds.

Drug-likeness and ADMET prediction

Drug-likeness evaluation has been conducted on 63 compounds using the web tool ADMESWISS, resulting in 34 compounds that passed the Lipinski rule of five (Table 1). The Lipinski Rule of Five is a widely used guideline to evaluate the drug-likeness of a compound, predicting its potential as an orally active drug in humans. This rule comes from studying molecules' Physicochemical properties, such as their molecular weight, hydrogen bond donors, hydrogen bond acceptors, and polar surface area [52,53].

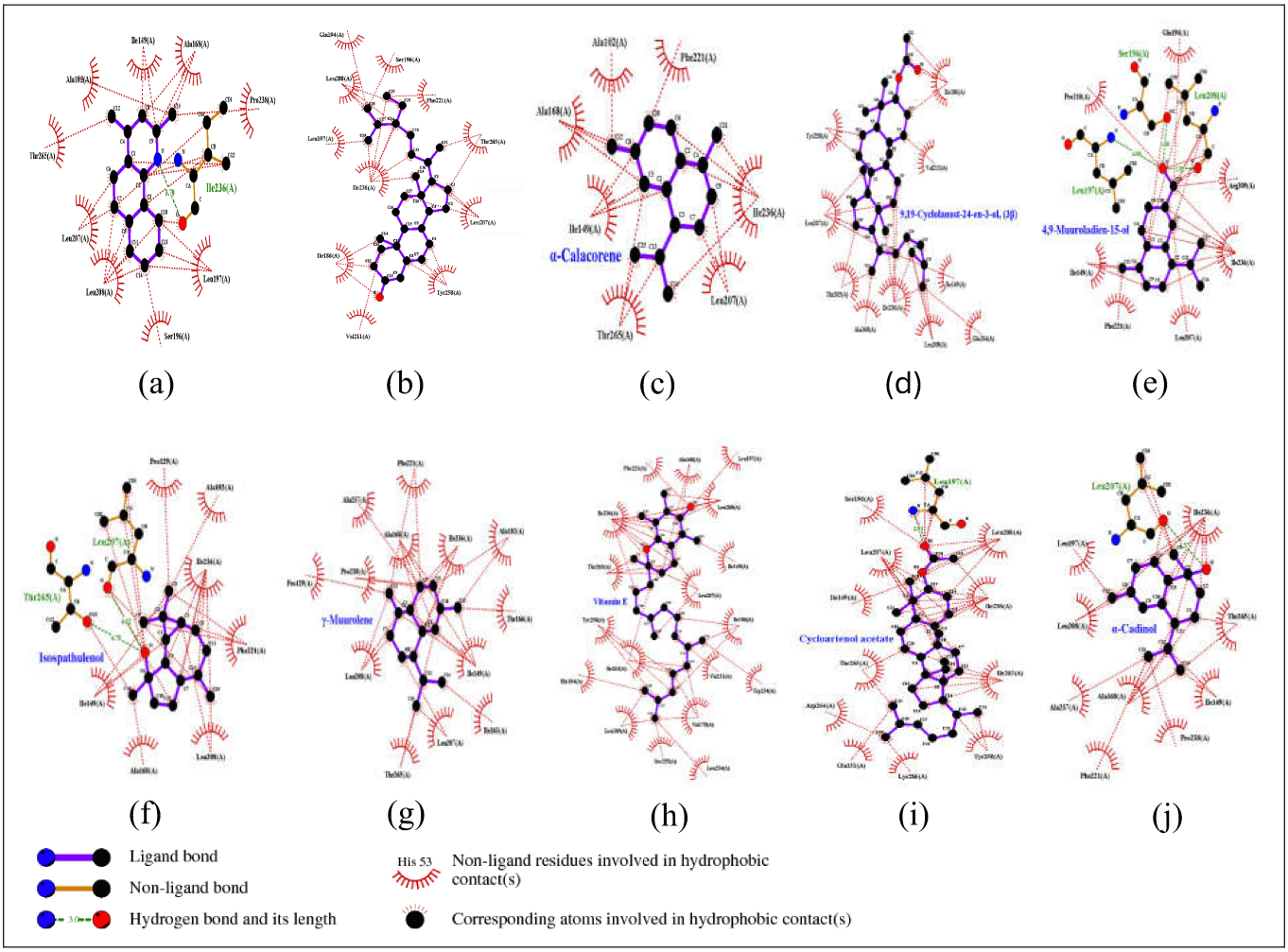

Figure 4. Visualization and interactions 2D amino acid of PqsR protein (PDB ID: 7P4U) with 10 compounds selected from NSL of *X. granatum* leaves. (a) Xg17; (b) Xg62; (c) Xg59; (d) Xg13; (e) Xg10; (f) Xg42; (g) Xg61; (h) Xg55; (i) Xg25; (j) Xg58.

Table 4. The interaction of PqsR receptor amino acid residues with the top ten compounds.

ID Comp.	Hydrophobic bonds	Hydrogen bonds
Xg17	Ser196, Leu197, Pro238, Ala168, Ile149, Ala102, Thr265, Leu207, Leu208	Ile236
Xg62	Tyr258, Leu207, Thr265, Phe221, Ser196, Gln194, Leu208, Leu197, Ile236, Ile186, Val211	-
Xg59	Ala102, Ile149, Ala168, Phe221, Ile236, Leu207, Thr265	-
Xg13	Ile186, Val211, Ile149, Gln194, Leu208, Ile236, Ala168, Thr265, Leu207	-
Xg10	Gln194, Arg209, Ile236, Leu207, Phe221, Ile149, Pro210	Leu208, Ser196, Leu197
Xg42	Pro129, Ala102, Ile236, Phe221, Leu208, Ala168, Ile149	Leu207, Thr265
Xg61	Phe221, Ala168, Ile236, Ala102, Thr166, Ile149, Ile263, Leu207, Thr265, Leu208, Pro129, Pro238, Ala237	-
Xg55	Phe221, Ala168, Leu197, Leu208, Ile149, Leu207, Ile186, Val211, Trp234, Val170, Leu254, Ser255, Leu189, His184, Ile263, Tyr258, Thr265, Ile236	Leu197
Xg25	Ser196, Leu207, Ile149, Thr265, Asp264, Glu151, Lys266, Tyr258, Ile263, Ile236, Leu208	-
Xg58	Ile236, Thr265, Ile149, Pro238, Ala168, Ala237, Leu208, Phe221, Leu197	Leu207

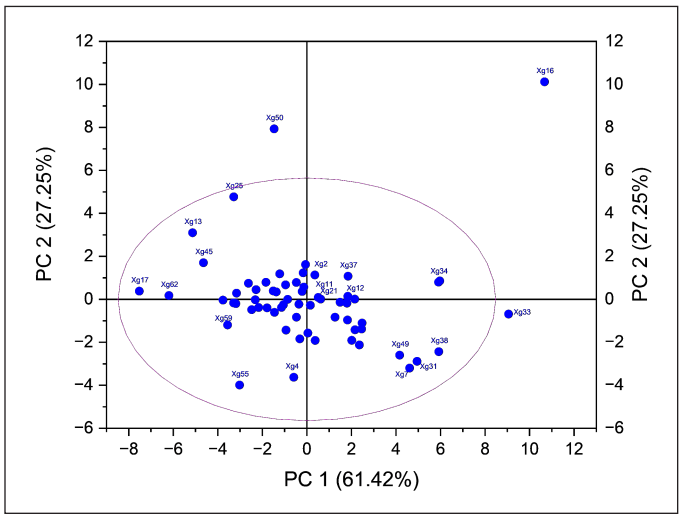

Figure 5. Distribution of PC loading values of 2-dimensional (6.a) and 3-dimensional plots of *X. granatum* leaf NSL with binding affinity docking values of LasI, LasR, and PqsR receptors, respectively.

The ability of 15 compounds to block the CYP1A2 enzyme could also stop the bioactivation of substances that cause cancer, especially those that are aromatic or heterocyclic amines. An amount of 34 compounds has the potential to inhibit the slow or rapid breakdown of drugs by the CYP2C19 enzyme [54].

Eight compounds have the potential to act as P–gp substrates. This resistance frequently arises in several disorders and is facilitated by multidrug transporters that aggressively expel drugs from cells, distancing them from their target areas [55].

The distribution of the ability to penetrate the skin layer includes 9 compounds in the strong category, 15 compounds in the moderate category, and 39 compounds in the weak category. Skin permeability (Kp) indicates the rate at which a chemical permeates the corneal layer. This value is commonly utilized to quantitatively characterize the movement of molecules in the outermost layer of the epidermis and to suggest the importance of skin absorption [56].

The digestive tract can absorb up to 31 compounds well, and the same number can cross the blood–brain barrier (BBB). Gastrointestinal (GI) absorption and BBB permeability are critical in drug development as they determine bioavailability and target site accessibility. GI absorption ensures an orally administered drug can enter systemic circulation effectively, influencing its bioavailability and therapeutic efficacy. High GI absorption is essential for oral drugs, while poor absorption limits effectiveness or necessitates alternative administration routes. BBB permeability, on the other hand, is crucial for central nervous system (CNS)-targeted drugs, as it allows them to reach the brain, overcoming the selective barrier protecting the CNS [57].

When compared to QS inhibitors derived from other plants, such as furanones, cinnamaldehyde, garlic, and polyphenolic compounds, their drug-likeness varies. Furanones, including natural furanones from *Delisea pulchra* and brominated furanones, are generally small and moderately lipophilic. Natural furanones demonstrate good drug-likeness, while brominated furanones may face solubility challenges due to their halogen content [58,59]. Cinnamaldehyde and its analogues have good drug-likeness, as they are small, lipophilic, and exhibit moderate LogP values, contributing to favorable absorption and solubility [60]. Garlic compounds, such as allicin and ajoene, have moderate drug-likeness, although allicin's instability and ajoene's bioavailability issues limit their potential as drug candidates despite their bioactivity [61,62]. Polyphenolic compounds**,** such as baicalin hydrate and epigallocatechin, typically exhibit poor drug-likeness due to their large molecular size and low bioavailability [63], although formulation strategies like nanoparticles or liposomes could improve their effectiveness. Overall, while some compounds demonstrate moderate drug-likeness, many would benefit from optimization or specialized delivery systems to overcome solubility and stability challenges [64].

Various formulation strategies, including structural modifications, nanoemulsion formulations, liposomal encapsulation, and co-administration with absorption enhancers, are being explored to improve the solubility, stability, and

bioavailability of these compounds. These approaches are aimed at enhancing their effectiveness as QS inhibitors [65–67].

CONCLUSION

TLs and nonsaponifiable lipids from *X. granatum* leave exhibit activity against the QSmechanisms of *P. aeruginosa* bacteria. Ten potent compounds, namely Xg17, Xg19, Xg13, Xg25, Xg42, Xg45, Xg55, Xg58, Xg59, and Xg62, effectively inhibit the activity of the LasR, LasI, and PqsR enzymes. They have potential as against resistant *P. aeruginosa*.

ACKNOWLEDGMENT

Thanks to the Research Centre for Chemistry, Indonesian Institute of Sciences-BRIN, PUSPIPTEK Serpong Area, Tangerang Selatan, Banten, Indonesia, for the scheme of doctoral student final project mentoring services.

AUTHOR CONTRIBUTIONS

All authors made significant contributions to the conception and design, data acquisition, or analysis and interpretation of data; participated in drafting the article or revising it critically for important intellectual content; agreed to submit the manuscript to the current journal; provided final approval of the version to be published; and are accountable for all aspects of the work. All authors meet the eligibility criteria for authorship in accordance with the International Committee of Medical Journal Editors (ICMJE) requirements/ guidelines.

CONFLICTS OF INTEREST

The authors report no financial or any other conflicts of interest in this work.

ETHICAL APPROVALS

This study does not involve experiments on animals or human subjects.

PUBLISHER'S NOTE

All claims expressed in this article are solely those of the authors and do not necessarily represent those of the publisher, the editors and the reviewers. This journal remains neutral with regard to jurisdictional claims in published institutional affiliation.

DATA AVAILABILITY

All data generated and analyzed during this study are provided within the research article.

USE OF ARTIFICIAL INTELLIGENCE (AI)-ASSISTED TECHNOLOGY

The authors declare that no artificial intelligence (AI) tools were used in the writing or editing of the manuscript, and no images were manipulated with AI.

REFERENCES

1. Sartelli M, Barie PS, Coccolini F, Abbas M, Abbo LM, Abdukhalilova GK, et al. Ten golden rules for optimal antibiotic use in hospital settings: the WARNING call to action. World J Emerg Surg. 2023 Oct 16;18(1):50.
2. Mancuso G, Midiri A, Gerace E, Biondo C. Bacterial antibiotic resistance: the most critical pathogens. Pathogens. 2021;10:1310.
3. Thakur M, Khushboo, Kumar Y, Yadav V, Pramanik A, Dubey KK. Understanding resistance acquisition by *Pseudomonas aeruginosa* and possible pharmacological approaches in palliating its pathogenesis. Biochem Pharmacol. 2023;215:115689. doi: https://doi.org/10.1016/j.bcp.2023.115689
4. WHO. The top 10 causes of death. WHO; 2020. 1 p.
5. Zhao X, Yu Z, Ding T. Quorum-sensing regulation of antimicrobial resistance in bacteria. Microorganisms. 2020 Mar 17;8(3):425.
6. Fan B, Li Y, Zhang Z, Yang Y, Li Y. Exploring cumulative vulnerability of mangrove forests to intensive coastal anthropogenic threats. Ecosystem Health Sustainability. 2024;10:1–11.
7. Darmadi J, Batubara RR, Himawan S, Azizah NN, Audah HK, Arsianti A, et al. Evaluation of Indonesian mangrove Xylocarpus granatum leaves ethyl acetate extract as potential anticancer drug. Sci Rep. 2021;11(1:1–18).
8. Dey D, Quispe C, Hossain R, Jain D, Ahmed Khan R, Janmeda P, et al. Ethnomedicinal use, phytochemistry, and pharmacology of *Xylocarpus granatum* J. Koenig. Evid Based Complement Alternat Med. 2021 Aug 30;2021:8922196.
9. Egra S, Hartini, Mardhiana, Nurjannah, Adiwena M, Santoso D, et al. Antibacterial and natural pesticide properties of Nyiri (*Xylocarpus granatum*). IOP Conf Ser Earth Environ Sci. 2022;1083:012020.
10. Seabra CL, Pinto RM, Nunes C, Reis S. Chapter 9 - Lipids as antimicrobials. In: Pintado M, Machado M, Gomes AM, Salsinha AS, Rodríguez-Alcalá LM, editors. Bioactive Lipids. Porto, Portugal: Academic Press; 2023. pp. 209–30. doi: https://doi.org/10.1016/B978-0-12-824043-4.00004-X
11. Peng X, Chen J, Gan Y, Yang L, Luo Y, Bu C, et al. Biofunctional lipid nanoparticles for precision treatment and prophylaxis of bacterial infections. Sci Adv. 2024;10(14):eadk9754. doi: https://doi.org/10.1126/sciadv.adk9754
12. Basyuni M, Wati R, Sagami H, Sumardi, Baba S, Oku H. Diversity and abundance of polyisoprenoid composition in coastal plant species from North Sumatra, Indonesia. Biodiversitas. 2018;19(1):1–11.
13. Wira Septama A, Arvia Chiara M, Turnip G, Nur Tasfiyati A, Triana Dewi R, Anggrainy Sianipar E, et al. Essential oil of *Zingiber cassumunar* Roxb. and *Zingiber officinaleRosc*.: a comparative study on chemical constituents, antibacterial activity, biofilm formation, and inhibition of *Pseudomonas aeruginosa* Quorum sensing system. Chem Biodivers. 2023;20(6):e202201205.
14. Septama A, Jantan I, Panichayupakaranant P, Aluwi M, Rahmi E. Immunosuppressive and antibacterial activities of dihydromorin and norartocarpetin isolated from Artocarpus heterophyllus heartwoods. Asian Pac J Trop Biomed. 2020;10(8):361–8.
15. Musthafa KS, Voravuthikunchai SP. Anti-virulence potential of eugenyl acetate against pathogenic bacteria of medical importance. Antonie van Leeuwenhoek Int J Gen Mol Microbiol. 2015;107(3):703–10.
16. Parmar GR, Shah AP, Sailor GU, Seth AK. *In silico* discovery of novel phytoconstituents of *Amyris pinnata* as a Mitotic Spindle Kinase Inhibitor. Curr Drug Res Rev. 2020;12(2):175–82.
17. Eberhardt J, Santos-Martins D, Tillack AF, Forli S. AutoDock Vina 1.2.0: new docking methods, expanded force field, and python bindings. J Chem Inf Model. 2021;61(8):3891–8.
18. Parmar G, Shah A, Shah S, Seth AK. Identification of bioactive phytoconstituents from the plant euphorbia hirta as potential inhibitor of sars-cov-2: An *in-silico* approach. Biointerface Res Appl Chem. 2022;12(2):1385–96.
19. Barnes V L, Heithoff DM, Mahan SP, House JK, Mahan MJ. Antimicrobial susceptibility testing to evaluate minimum inhibitory concentration values of clinically relevant antibiotics. STAR Protoc. 2023;4(3):102512. doi: https://doi.org/10.1016/j.xpro.2023.102512
20. Kowalska-Krochmal B, Dudek-Wicher R. The minimum inhibitory concentration of antibiotics: methods, interpretation, clinical relevance. Pathogens. 2021 Feb 4;10(2):165.

21. Woo S, Marquez L, Crandall WJ, Risener CJ, Quave CL. Recent advances in the discovery of plant-derived antimicrobial natural products to combat antimicrobial resistant pathogens: insights from 2018–2022. Nat Prod Rep. 2023;40(7):1271–90. doi: https://doi.org/10.1039/D2NP00090C
22. Alves E, Dias M, Lopes D, Almeida A, Domingues MDR, Rey F. Antimicrobial lipids from plants and marine organisms: an overview of the current state-of-the- art and future prospects. Antibiotics. 2020;9:1–88.
23. Gopalakrishnan AV, Kanagaraja A, Sakthivelu M, Devadasan V, Gopinath SCB, Raman P. Role of fatty acids in modulating quorum sensing in *Pseudomonas aeruginosa* and *Chromobacterium violaceum*: an integrated experimental and computational analysis. Int Microbiol. 2024. doi: https://doi.org/10.1007/s10123-024-00590-y
24. Kearns DB. A field guide to bacterial swarming motility. Nat Rev Microbiol. 2010;8:634–44.
25. Passarinho PC, Oliveira B, Dias C, Teles M, Reis A, Lopes da Silva T. Sequential carotenoids extraction and biodiesel production from *Rhodosporidium toruloides* NCYC 921 biomass. Waste Biomass Valorization. 2020;11(5):2075–86.
26. Panda AK, De Mandal S, Shakeel M, Bisht SS, Khan J. Natural anti-biofilm agents: strategies to control biofilm-forming pathogens. Front Microbiol. 2020;11:1–23. doi: https://doi.org/10.3389/fmicb.2020.566325
27. Ghssein G, Ezzeddine Z. A Rreview of *Pseudomonas aeruginosa* metallophores: pyoverdine, Ppyochelin and pseudopaline. Biology. 2022;11:1711.
28. Mudaliar SB, Bharath Prasad AS. A biomedical perspective of pyocyanin from *Pseudomonas aeruginosa*: its applications and challenges. World J Microbiol Biotechnol. 2024 Feb 10;40(3):90.
29. Khan F. Multifaceted strategies for alleviating *Pseudomonas aeruginosa* infection by targeting protease activity: natural and synthetic molecules. Int J Biol Macromol. 2024;278:134533. doi: https://doi.org/10.1016/j.ijbiomac.2024.134533
30. Kasthuri T, Barath S, Nandhakumar M, Karutha Pandian S. Proteomic profiling spotlights the molecular targets and the impact of the natural antivirulent umbelliferone on stress response, virulence factors, and the quorum sensing network of *Pseudomonas aeruginosa*. Front Cell Infect Microbiol. 2022 Nov 30;12:998540. doi: https://doi.org/10.3389/fcimb.2022.998540
31. Sá S, Silva C, Dias MC, Veiga M, Lopes S, Fernandes R, et al. Virulence-linked mutations in rubredoxin reductase and glutaredoxin: impact on antibiotic susceptibility and phage therapy in *Pseudomonas aeruginosa*. Applied Sciences (Switzerland). 2023;13(21):11918. doi: https://doi.org/10.3390/app132111918
32. Rahman A, Sardar S, Niaz Z, Khan A, Sheheryar S, Alrefaei AF, et al. Lipase and protease production ability of multi-drug resistant bacteria worsens the outcomes of wound infections. Curr Pharm Des. 2024;30(17):1307–16. doi: https://doi.org/10.2174/0113816128302189240402043330
33. Gad AI, El-Ganiny AM, Eissa AG, Noureldin NA, Nazeih SI. Miconazole and phenothiazine hinder the quorum sensing regulated virulence in *Pseudomonas aeruginosa*. J Antibiotics. 2024;77(7):454–65. doi: https://doi.org/10.1038/s41429-024-00731-5
34. Gyrdymova Y V, Rubtsova SA. Caryophyllene and caryophyllene oxide: a variety of chemical transformations and biological activities. Chem Papers. 2022;76(1):1–39. doi: https://doi.org/10.1007/s11696-021-01865-8
35. Lü X, Zhang Y, Yang L, Chen A, Zhang Z, Shen G. Antibiofilm activity of d-limonene against spoilage *Bacillus amyloliquefaciens*. Food Biosci. 2024;61:104568. doi: https://doi.org/10.1016/j.fbio.2024.104568
36. Rütschlin S, Böttcher T. Inhibitors of bacterial swarming behavior. Chemistry 2020;26:964–79.
37. Qaralleh H, Saghir SAM, Al-limoun MO, Dmor SM, Khleifat K, Al-Ahmad BEM, *et al.* Effect of *Matricaria aurea* essential oils on biofilm development, virulence factors and quorum sensing-dependent genes of *Pseudomonas aeruginosa*. Pharmaceuticals 2024;17(3):386.
38. Soltani S, Bazzaz BSF, Hadizadeh F, Roodbari F, Soheilic V. New insight into vitamins E and K1 as anti-quorum-sensing agents against *Pseudomonas aeruginosa*. Antimicrob Agents Chemother. 2021;65(6):e01342. doi: https://doi.org/10.1128/AAC.01342-20
39. Sharifi-Rad M, Varoni EM, Salehi B, Sharifi-Rad J, Matthews KR, Ayatollahi SA, *et al.* Plants of the genus zingiber as a source of bioactive phytochemicals: from tradition to pharmacy. Molecules 2017;22(12):2145.
40. Çevikbaş H, Ulusoy S, Kaya Kinaytürk N. Exploring rose absolute and phenylethyl alcohol as novel quorum sensing inhibitors in *Pseudomonas aeruginosa* and *Chromobacterium violaceum*. Sci Rep. 2024;14(1):15666. doi: https://doi.org10.1038/s41598-024-66888-z
41. Chadha J, Moudgil G, Harjai K. Synergism between α-terpineol and terpinen-4-ol potentiates antivirulence response against *Pseudomonas aeruginosa*. Indian J Microbiol. 2024;64:1951–5. doi: https://doi.org/10.1007/s12088-024-01189-7
42. El Gendy AENG, Essa AF, El-Rashedy AA, Elgamal AM, Khalaf DD, Hassan EM, *et al.* Antiviral potentialities of chemical characterized essential oils of *Acacia nilotica* bark and fruits against hepatitis A and herpes simplex viruses: *in vitro*, in silico, and molecular dynamics studies. Plants 2022;11(21):2889. doi: https://doi.org10.3390/plants11212889
43. Shariati A, Noei M, Askarinia M, Khoshbayan A, Farahani A, Chegini Z. Inhibitory effect of natural compounds on quorum sensing system in *Pseudomonas aeruginosa*: a helpful promise for managing biofilm community. Front Pharmacol. 2024;15:1350391.
44. Almeida FCL, Sanches K, Pinheiro-Aguiar R, Almeida VS, Caruso IP. Protein surface interactions—theoretical and experimental studies. Front Mol Biosci. 2021;8:706002. doi: /https://doi.org/10.3389/fmolb.2021.706002
45. Agu PC, Afiukwa CA, Orji OU, Ezeh EM, Ofoke IH, Ogbu CO, *et al.* Molecular docking as a tool for the discovery of molecular targets of nutraceuticals in diseases management. Sci Rep. 2023;13(1):13398. doi: https://doi.org/10.1038/s41598-023-40160-2
46. O'Loughlin CT, Miller LC, Siryaporn A, Drescher K, Semmelhack MF, Bassler BL. A quorum-sensing inhibitor blocks *Pseudomonas aeruginosa* virulence and biofilm formation. Proc Natl Acad Sci U S A. 2013;110(44):17981–6. doi: https://doi.org/10.1073/pnas.1316981110
47. Wang C, Chen Y, Zhang Y, Li K, Lin M, Pan F, *et al.* A reinforcement learning approach for protein–ligand binding pose prediction. BMC Bioinformatics 2022;23(1):368. doi: https://doi.org/10.1186/s12859-022-04912-7
48. Gould TA, Schwelzer HP, Churchill MEA. Structure of the *Pseudomonas aeruginosa* acyl-homoserilactone synthase LasI. Mol Microbiol. 2004;53(4):1135–46.
49. Schütz C, Empting M. Targeting the *Pseudomonas quinolone* signal quorum sensing system for the discovery of novel anti-infective pathoblockers. Beilstein J Org Chem. 2018;14:2627–45.
50. Sullivan JH, Warkentin M, Wallace L. So many ways for assessing outliers: what really works and does it matter? J Bus Res. 2021;132:530–43. doi: https://doi.org/10.1016/j.jbusres.2021.03.066
51. Li Q, Mao S, Wang H, Ye X. The molecular architecture of *Pseudomonas aeruginosa* quorum-sensing inhibitors. Marine Drugs 2022;20(8):488.
52. Lipinski CA, Lombardo F, Dominy BW, Feeney PJ. Experimental and computational approaches to estimate solubility and permeability in drug discovery and development settings. Adv Drug Deliv Rev. 1997;23(1):3–25. doi: https://doi.org/10.1016/S0169-409X(96)00423-1

53. Leeson PD, Springthorpe B. The influence of drug-like concepts on decision-making in medicinal chemistry. Nat Rev Drug Discov. 2007;6(11):881–90. doi: https://doi.org/10.1038/nrd2445
54. Zhao M, Ma J, Li M, Zhang Y, Jiang B, Zhao X, *et al.* Cytochrome P450 enzymes and drug metabolism in humans. Int J Mol Sci. 2021;22(23):12808. doi: https://doi.org/10.3390/ijms222312808
55. Ahmed Juvale II, Abdul Hamid AA, Abd Halim KB, Che Has AT. P-glycoprotein: new insights into structure, physiological function, regulation and alterations in disease. Heliyon 2022;8(6):e09777. doi: https://doi.org/10.1016/j.heliyon.2022.e09777
56. Chen CP, Chen CC, Huang CW, Chang YC. Evaluating molecular properties involved in transport of small molecules in stratum corneum: a quantitative structure-activity relationship for skin permeability. Molecules 2018;23(4):911. doi: https://doi.org/10.3390/molecules23040911
57. Fu BM, Zhao Z, Zhu D. Blood-brain barrier (BBB) permeability and transport measurement *in vitro* and *in vivo*. In: Turksen K, editor. Permeability barrier: methods and orotocols. New York, NY: Springer US; 2021. pp. 105–22. doi: https://doi.org/10.1007/7651_2020_308
58. Husain A, Khan SA, Iram F, Iqbal MA, Asif M. Insights into the chemistry and therapeutic potential of furanones: a versatile pharmacophore. Eur J Med Chem. 2019;171:66–92. doi: https://doi.org/10.1016/j.ejmech.2019.03.021
59. Muñoz-Cázares N, Castillo-Juárez I, García-Contreras R, Castro-Torres VA, Díaz-Guerrero M, Rodríguez-Zavala JS, *et al.* A brominated furanone inhibits *Pseudomonas aeruginosa* quorum sensing and type III secretion, attenuating its virulence in a murine cutaneous abscess model. Biomedicines 2022;10(8):1847. doi: https://doi.org/10.3390/biomedicines10081847
60. Brackman G, Celen S, Hillaert U, van Calenbergh S, Cos P, Maes L, *et al.* Structure-activity relationship of cinnamaldehyde analogs as inhibitors of AI-2 based quorum sensing and their effect on virulence of *Vibrio* spp. PLoS One 2011;6(1):e16084.
61. Deng Y, Ho CT, Lan Y, Xiao J, Lu M. Bioavailability, health benefits, and delivery systems of allicin: a review. J Agric Food Chem. 2023;71(49):19207–20. doi: https://doi.org/10.1021/acs.jafc.3c05602
62. Zhou S, Yan X, Qiao X, Qiu Z, Zhu W, Lu X, *et al.* Evaluate the stability of synthesized allicin and its reactivity with endogenous compounds in garlic. NPJ Sci Food. 2025;9(1):18. doi: https://doi.org/10.1038/s41538-025-00374-2
63. Andreu Fernández V, Almeida Toledano L, Pizarro Lozano N, Navarro Tapia E, Gómez Roig MD, la Torre Fornell R, *et al.* Bioavailability of epigallocatechin gallate administered with different nutritional strategies in healthy volunteers. Antioxidants 2020;9(5):440. doi: https://doi.org/10.3390/antiox9050440
64. Brackman G, Coenye T. Quorum sensing inhibitors as anti-biofilm agents. Curr Pharm Des. 2015;21(1):5–11.
65. Kumari L, Choudhari Y, Patel P, Gupta GD, Singh D, Rosenholm JM, *et al.* Advancement in solubilization approaches: a step towards bioavailability enhancement of poorly soluble drugs. Life 2023;13(5):1099. doi: https://doi.org/10.3390/life13051099
66. Hu Y, Zhang L, Wei LF, Lu FY, Wang LH, Ding Q, *et al.* Liposomes encapsulation by pH driven improves the stability, bioaccessibility and bioavailability of urolithin A: a comparative study. Int J Biol Macromol. 2023;253:127554. doi: https://doi.org/10.1016/j.ijbiomac.2023.127554
67. Ashfaq R, Rasul A, Asghar S, Kovács A, Berkó S, Budai-Szűcs M. Lipid nanoparticles: an effective tool to improve the bioavailability of nutraceuticals. Int J Mol Sci. 2023;24(21):15764. doi: https://doi.org/10.3390/ijms242115764

How to cite this article:
Sumardi S, Masfria M, Basyuni M, Septama AW. Quorum sensing inhibitory potential and molecular docking study of lipid extract from *Xylocarpus granatum* leaves against *Pseudomonas aeruginosa*. J Appl Pharm Sci. 2025;15(07):203–219. DOI: 10.7324/JAPS.2025.231809